NANO EXPRESS

Open Access

One-pot synthesis of monodisperse CoFe₂O₄@Ag core-shell nanoparticles and their characterization

Shuta Hara[1], Jumpei Aisu[1], Masahiro Kato[1], Takashige Aono[2], Kosuke Sugawa[1], Kouichi Takase[2], Joe Otsuki[1], Shigeru Shimizu[1] and Hiroki Ikake[1*]

Abstract

In recent years, monodispersed magnetic nanoparticles with a core/shell structure are expected for their wide applications including magnetic fluid, recoverable catalysts, and biological analysis. However, their synthesis method needs numerous processes such as solvent substitution, exchange of protective agents, and centrifugation. A simple and rapid method for the synthesis of monodispersed core-shell nanoparticles makes it possible to accelerate their further applications. This paper describes a simple and rapid one-pot synthesis of core (CoFe₂O₄)-shell (Ag) nanoparticles with high monodispersity. The synthesized nanoparticles showed plasmonic light absorption owing to the Ag shell. Moreover, the magnetic property of the nanoparticles had a soft magnetic behavior at room temperature and a hard magnetic behavior at 5 K. In addition, the nanoparticles showed high monodispersity with a low polydispersity index (PDI) value of 0.083 in hexane.

Keywords: Core-shell nanoparticles, Cobalt ferrite, Supermagnetism, Surface plasmon resonance

Background

Over the last decade, magnetic nanoparticles with a core/shell structure have gained a lot of attention in a wide range of fields from engineering to medical sciences owing to the applications of magnetic fluids [1, 2], magnetic separation [1–3], recoverable catalysts [1, 2, 4–7], drug delivery system [1, 8–10], and an enhanced magnetic resonance imaging (MRI) contrast agents [7, 9–11].

Among the magnetic nanoparticles, a spinel ferrite nanoparticle has frequently been employed as a magnetic core because of its excellent magnetic and electrical properties [12]. Particularly, cobalt ferrite (CoFe₂O₄) nanoparticles have a large maximum coercive field (H_c), even with a small size as well as a remarkable chemical stability and a mechanical hardness [13–17]. Although many different chemical methods have been developed to fabricate CoFe2O4 nanoparticles, the thermal decomposition method has recently been employed one of the most promising procedures to obtain highly, structurally, and morphologically controlled nanoparticles with a high crystallinity [13, 17, 18].

Magnetic nanoparticles with a core/shell structure have attracted a great deal of attention due to their multifunctionality including optical, electronic, and magnetic properties [6, 8, 10, 19]. In particular, the Au shell-coated magnetic nanoparticles have widely been studied in order to provide not only the surface plasmon properties but also a reactive surface for strong binding to organic compounds containing thiol groups [3, 20]. Typically, an approach of combined two-step thermal decomposition process can continuously synthesize from cores to shells, resulting in the formation of Au-coated magnetic nanoparticles with a high monodispersity [20]. On the other hand, Ag shell-coated magnetic nanoparticles have not been synthesized by this approach in spite of excellent plasmonic properties, a higher extinction coefficient, a sharper extinction band, a higher light scattering-to-extinction effect, and strong local electromagnetic fields of Ag shells.

* Correspondence: ikake.hiroki@nihon-u.ac.jp
[1]Department of Materials and Applied Chemistry, College of Science and Technology, Nihon University, 1-8-14 Kandasurugadai, Chiyoda-ku, Tokyo 101-8308, Japan
Full list of author information is available at the end of the article

Hara *et al. Nanoscale Research Letters* (2018) 13:176

Page 2 of 7

In this study, we succeeded in synthesizing Ag shell-coated $CoFe_2O_4$ nanoparticles by a simple and rapid one-pot method involving two thermal decomposition processes. It was confirmed that our synthesized nanoparticles formed a precise core-shell structure, as compared with those synthesized in a previous paper [21, 22]. In addition, we demonstrated that the $CoFe_2O_4@Ag$ showed the localized surface plasmon resonance (LSPR) originated from the Ag shells. In the investigation of the magnetic property, this core-shell nanoparticle revealed soft magnetic behavior with H_c of 70 Oe at 300 k and hard magnetic behavior with 11 k Oe at 5 K.

Method/Experimental

Material

$Fe(acac)_3$ and $Co(acac)_2$ were purchased from Tokyo Chemical Industry. Diphenyl ether, oleylamine (OAm), and silver(I) acetate were purchased from Wako. Oleic acid (OA) was purchased from Kanto Chemical.

Synthesis of CoFe2O4@Ag

The CoFe2O4@Ag were synthesized by the two-step high thermal decomposition method (Scheme 1). $Fe(acac)_3$ (0.353 g, 1 mmol), $Co(acac)_2$ (0.129 g, 0.5 mmol), and OA (3.39 g, 12 mmol) were dissolved in 30 mL of diphenyl ether, which was pre-treated by heating at 180 °C for 30 min. A mixture was heated at 180 °C for 16 h under vigorous stirring. The solution color gradually turned from dark red to fine black. After cooling at room temperature, a mixture of OA (1.48 g, 5.2 mmol), OAm (8.13 g, 30.4 mmol), and silver acetate (0.61 g, 3.6 mmol) dissolved in 100 mL of diphenyl ether was added to the mixture, followed by heating at 180 °C for 1.5 h. The color of the mixture further turned to metallic dark purple during heating. After cooling, 400 mL of methanol as a poor solvent was added to the mixture solution, followed by centrifugation (5000 rpm, 5 min) and the redispersion in 60 mL of hexane. Although the nanoparticles dispersed in the solution might be able to be magnetically separated, it takes time to recover. The centrifugation process was repeated several times to remove the unreacted precursors. Finally, by centrifuging the colloidal hexane solution (14,000 rpm, 20 min), the resulting precipitates were removed. The net weight of nanoparticles by this method is about 60 mg as 1 mg/mL of the colloidal hexane solution. The $CoFe_2O_4$ nanoparticles as a reference were prepared by performing only step 1 in Scheme 1.

Characterization and Calculation

The morphology of nanoparticles was observed using field-emission transmission electron microscopy (TEM) (Hitachi, Ltd., FE 2000). The crystal structures were measured with X-ray diffraction (XRD) (PANalytical, X'Pert PRO MPD) in the range of $2\theta = 20°$ to $80°$ by using the CuK α-ray. Element composition of nanoparticles was analyzed by X-ray photoelectron spectroscopy (XPS) (KARATOS ESCA 3400). Etching operation was performed with Ar ion gun. The magnetization measurements were performed by a superconducting quantum interference device (SQUID) (Cryogenic, S700X-R). The optical properties were measured on a UV-visible spectrophotometer (Jasco, V-670). Dynamic light scattering (DLS) (Malvern, zetasizer-nano-zs) was measured with 633-nm laser line. For the optical properties of our synthesized core-shell nanoparticles, the experimental data are supported by Mie scattering calculations which were carried out by Bohren and Huffman's solution [23] using the MATLAB code written by Mätzler [24]. Dielectric functions for the Ag were taken from Reference [25].

Results and Discussion

Figure 1 shows the TEM images of $CoFe_2O_4$ nanoparticles and $CoFe_2O_4@Ag$ core-shell nanoparticles. As shown in the insets of Fig. 1, the size distributions of both nanoparticles are narrow. The average sizes (mean ± S.D.) of them are 3.5 ± 0.76 and 5.5 ± 0.77 nm, respectively. From these results, the thickness of Ag shell was estimated to be ca. 1 nm. Aggregation of $CoFe_2O_4$ particles occurred but not for $CoFe_2O_4@Ag$ nanoparticles. This is possibly due to a
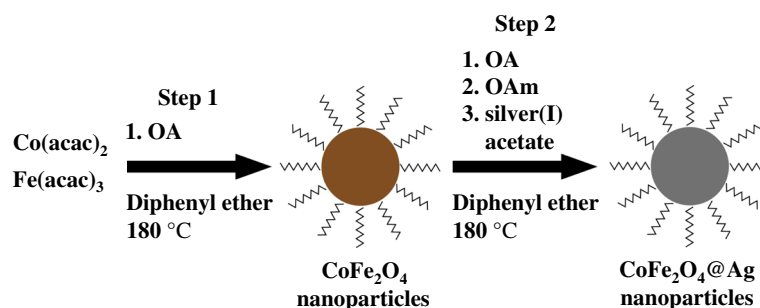
Scheme 1 Procedure for synthesizing $CoFe_2O_4@Ag$ nanoparticles

Hara *et al. Nanoscale Research Letters* (2018) 13:176

Page 3 of 7

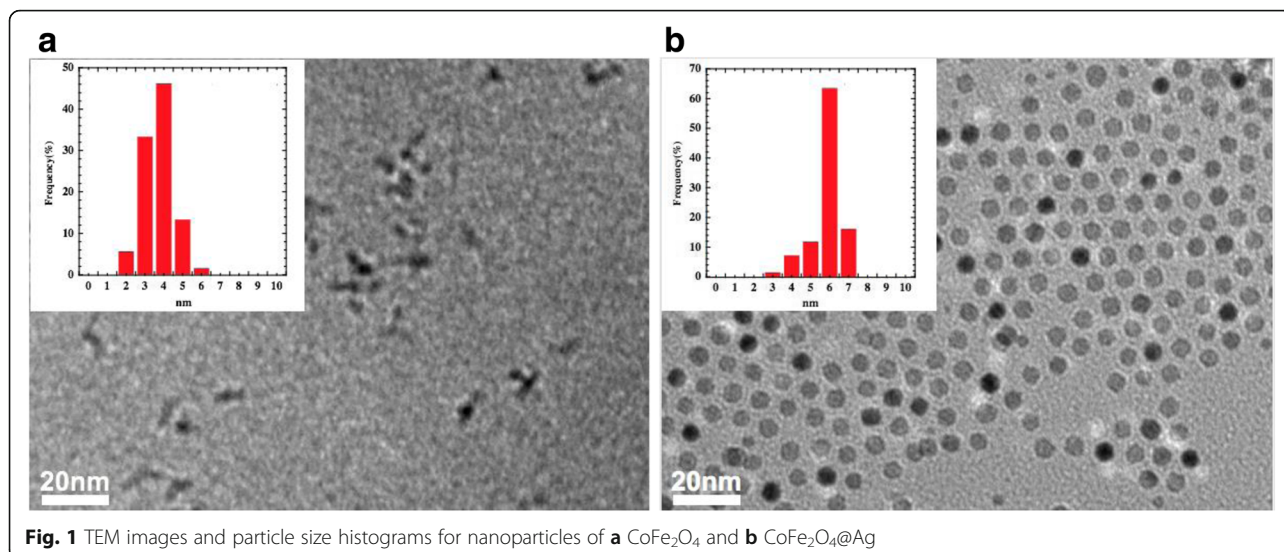**Fig. 1** TEM images and particle size histograms for nanoparticles of **a** CoFe$_2$O$_4$ and **b** CoFe$_2$O$_4$@Ag

higher surface energy of the CoFe2O4 nanoparticles than that of the CoFe$_2$O$_4$@Ag nanoparticles because of a larger surface-to-volume ratio of the CoFe$_2$O$_4$ nanoparticles [26]. Also, residual CoFe$_2$O$_4$ nanoparticles (cores) could not be observed in the sample of CoFe$_2$O$_4$@Ag. This result suggests that almost all the cores are uniformly coated with the silver Ag shell.

Figure 2 presents the XRD patterns for the CoFe$_2$O$_4$ and the CoFe$_2$O$_4$@Ag nanoparticles. The diffraction peaks of CoFe$_2$O$_4$ nanoparticles at 2θ = 30.50°, 35.75°,

43.50°, 53.8°, 57.5°, 63.0°, and 74.4° show the formation of a single crystallographic phase, which can be indexed as the cubic structure of spinel oxides [17]. On the other hand, the diffraction peaks of CoFe$_2$O$_4$@Ag at 2θ = 38.42°, 44.50°, 64.91°, 77.75°, and 81.83° correspond to those of the standard face-centered cubic (fcc) phase of Ag [10]. The intensity of the diffraction peaks of CoFe$_2$O$_4$ are relatively weak, and its main peak overlaps with Ag; therefore, all emerge into those of Ag. The crystallite size was calculated from the full width at half maximum (FWHM) of the highest intensity diffraction peak, which is based on the Debye-Scherrer equation,

$$t = 0.9l/b \ \cos y \qquad (1)$$

where t is the crystallite size, l is the wavelength of Cu-Ka radiation, b is the FWHM, and y is the diffraction angle of the strongest peak. The crystal sizes evaluated from the diffraction patterns were 7.1 and 3.6 nm for CoFe$_2$O$_4$ nanoparticles and CoFe$_2$O$_4$@Ag nanoparticles, respectively. The crystal size of CoFe$_2$O$_4$ nanoparticles was observed to be larger than the size of TEM because of the residue of CoFe$_2$O$_4$ nanoparticles out of size distribution, which could not be removed by centrifugation in hexane. On the other hand, the crystal size from XRD showed an agreement in CoFe2O4@Ag nanoparticles considering that the crystal size of Ag shell has to be smaller than the size of TEM. The size of the colloid after the silver coating reaction enables to select by centrifugation due to its heavyweight in hexane.

To evaluate the internal composition of the obtained nanoparticles with a core-shell structure, the nanoparticle surfaces were etched using Ar ion gun in the chamber [27]. According to the previous studies, when the
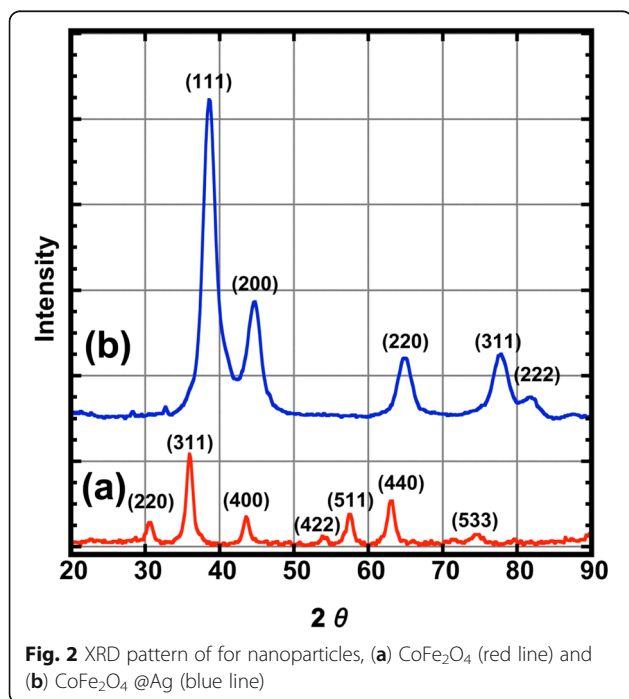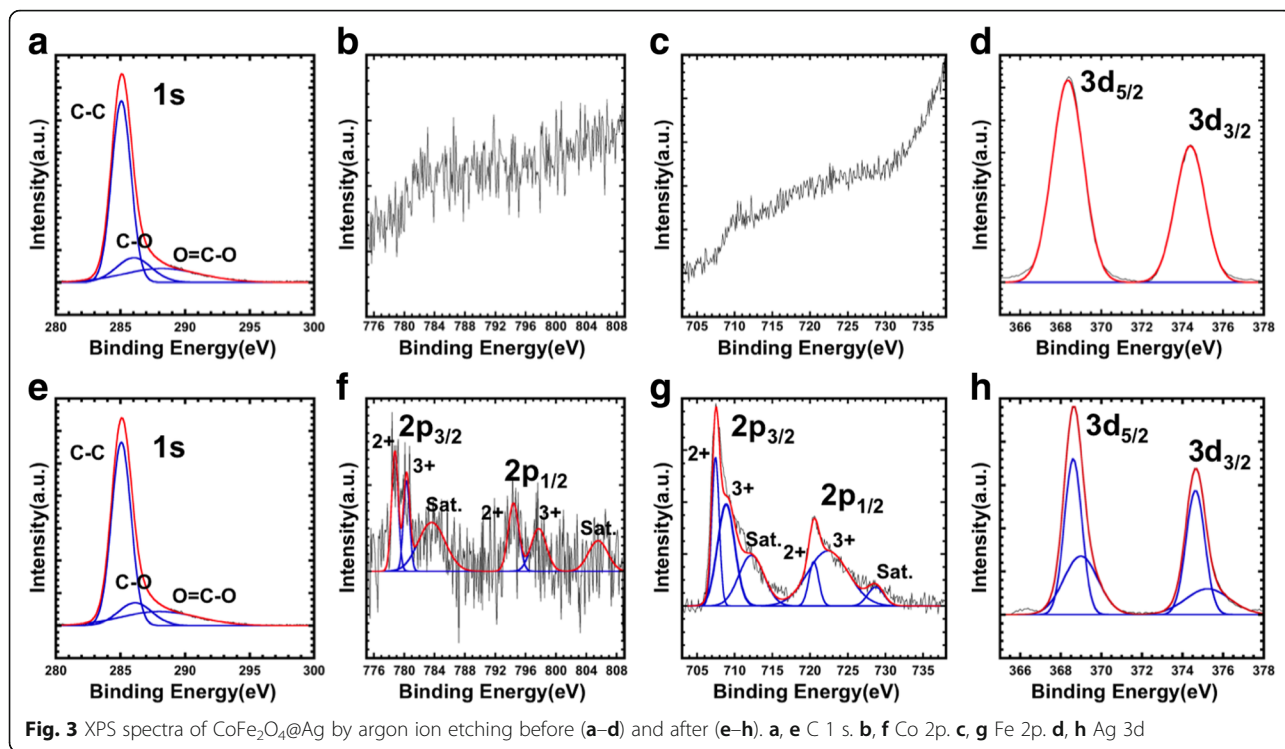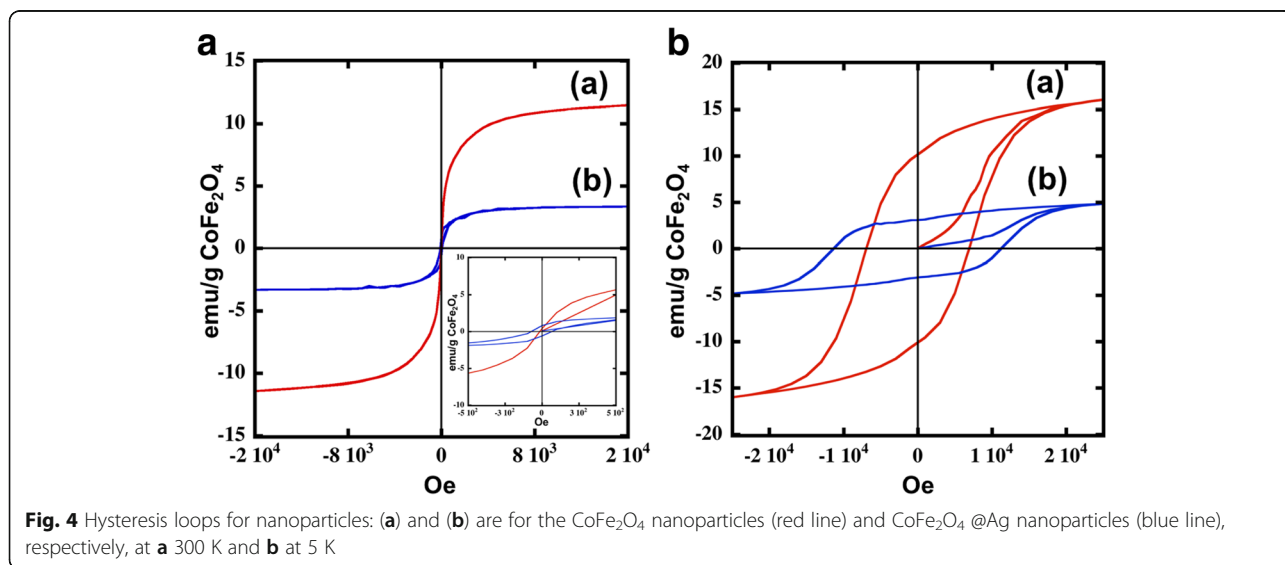

Fig. 2 XRD pattern of for nanoparticles, (**a**) CoFe$_2$O$_4$ (red line) and (**b**) CoFe$_2$O$_4$ @Ag (blue line)

Hara *et al. Nanoscale Research Letters* (2018) 13:176

Page 4 of 7

Fig. 3 XPS spectra of CoFe$_2$O$_4$@Ag by argon ion etching before (**a–d**) and after (**e–h**). **a**, **e** C 1 s. **b**, **f** Co 2p. **c**, **g** Fe 2p. **d**, **h** Ag 3d

particles had a precise core-shell structure, the peak intensity of the element contained in the core should be increased as the etching progresses. As shown in Fig. 3a–d, to determine the surface composition of CoFe$_2$O$_4$@Ag nanoparticles, we measured the XPS spectra before the Ar ion etching. In the initial surfaces, the peek C (1 s) were easily observed in nanoparticles due to the presence of the protective agent on the surface of the nanoparticles (Fig. 3a). The spectrum of C (1 s) was decomposed, and a peak

derived from C-O-C was observed, which is derived from oleic acid modified on the surface. While the peaks of Ag(3d) were observed, those of Fe(2p) and Co(2p) could not be observed, indicating that the core was completely covered with the Ag shells (Fig. 3b–d). On the other hand, the peaks of Fe(2p) and Co(2p) were observed in the nanoparticles after the etching operation with argon ion (Fig. 3f, g). The peaks of Fe(2p) and Co(2p) are decomposed and can be assigned to Fe^{2+}, Fe^{3+}, Co^{2+}, and Co^{3+},

Fig. 4 Hysteresis loops for nanoparticles: (**a**) and (**b**) are for the CoFe$_2$O$_4$ nanoparticles (red line) and CoFe$_2$O$_4$ @Ag nanoparticles (blue line), respectively, at **a** 300 K and **b** at 5 K

Hara et al. Nanoscale Research Letters (2018) 13:176

Page 5 of 7

respectively. The formation of both types of charge carriers results from the loss of oxygen during the high-temperature reaction process [28, 29]. For the charge compensation, a part of Fe3+ is converted to Fe2+, and a part of Co2+ is converted to Co3+. Furthermore, each of the Ag(3d) peak after the etching can be decomposed into two peaks (Fig. 3h), due to the difference in electronic state at between the nanoparticle surfaces and the inside of the shells. These results indicate that the precise core-shell structure is formed.

The magnetic hysteresis loops of films made up of the $CoFe_2O_4$ and the $CoFe_2O_4@Ag$ nanoparticles were measured at 300 and 5 K, as shown in Fig. 4. These hysteresis loops were normalized as the magnetic susceptibility per unit cobalt weight. Due to the analysis of the crystallographic phase using XRD (Fig. 2), the crystalline densities of $CoFe_2O_4$ and $CoFe_2O_4@Ag$ nanoparticles were estimated to be 5.3 and 10.5 g/cm^3, respectively. Also, the volumes of $CoFe_2O_4$ and $CoFe_2O_4@Ag$ nanoparticles were calculated using the results from the TEM observation (Fig. 1). $CoFe_2O_4$ nanoparticles showed a superparamagnetic behavior at room temperature (Fig. 4a). As mentioned by López-Ortega et al. [17], the $CoFe_2O_4$ nanoparticles with the size below 20 nm showed the superparamagnetic behavior at room temperature. The magnetic properties of each sample at the two temperatures are summarized in Table 1. Magnetic saturation (M_s) of the $CoFe_2O_4$ nanoparticles was 11 (emu/g $CoFe_2O_4$), which is lower than the previous results [17, 30, 31]. This is possibly owing to the smaller particle size obtained in this study. On the other hand, the M_s of the $CoFe_2O_4@Ag$ was even smaller with a value of 3.3 (emu/g, $CoFe_2O_4$). As mentioned in the previous literature for $Fe_3O_4@Ag$ nanoparticles [8–10, 32–34], the M_s of $CoFe_2O_4@Ag$ decreases possibly due to the diamagnetic contribution of the Ag shell. Moreover, $CoFe_2O_4@Ag$ showed 77 Oe, which is high H_c value at 300 k. The H_c of the $CoFe_2O_4@Ag$ is also different from that of $CoFe_2O_4$ under the low temperature (Fig. 4b). Both of the nanoparticles exhibited ferromagnetism at 5 K despite their relatively small sizes. On the basis of the data near zero magnetization, the value of H_c increases for $CoFe_2O_4@Ag$ nanoparticles (7 k Oe for $CoFe_2O_4$ and

11 k Oe for $CoFe_2O_4@Ag$). This interesting behavior has also been observed in other core-shell nanoparticles such as Fe@Ag [10] and $Fe_3O_4@Au$ nanoparticles [5]. Taking these facts into account, the increase of the H_c of the $CoFe_2O_4@Ag$ nanoparticles can be derived from a less-effective coupling of magnetic dipole moment [5, 20].

Next, optical properties of the $CoFe_2O_4$ nanoparticles were investigated by UV-visible spectral measurements. Ag nanoparticles are known to show significant light extinction in the visible region due to the excitation of localized surface plasmon resonance (LSPR) by the coupling of the irradiated light with the coherent oscillation of surface electrons within the Ag nanoparticles. Although the $CoFe_2O_4$ nanoparticles showed no LSPR extinction band in the visible region (Fig. 5), the colloidal solution of our core-shell type $CoFe_2O_4@Ag$ nanoparticles showed a sharp extinction peak at 416 nm. This can be attributed to the plasmon absorption (dipole mode) of the Ag shell, which is theoretically supported by the Mie theory (see Additional file 1). This interesting behavior has been observed for Fe@Ag nanoparticles [10] and Co@Ag nanoparticles [7]. In addition, the spectroscopic properties of the $CoFe_2O_4@Ag$ nanoparticles were not changed for 1 month, indicating the superior stability of the nanoparticles under air.

The colloidal stability of the $CoFe_2O_4$ and the $CoFe_2O_4@Ag$ nanoparticles was evaluated by measuring the size distributions of the nanoparticles in hexane using DLS (Fig. 6). The average sizes of the $CoFe_2O_4$ and $CoFe_2O_4@Ag$ nanoparticles were measured to be 19.67 and 9.27 nm, respectively. The sizes of these

Table 1 Magnetic properties of CoFe$_2$O$_4$ nanoparticles and CoFe$_2$O$_4$@Ag nanoparticles

Nanoparticle	M_s (5 k) (emu/g, CoFe204)	H_c (5 k) (KOe)	Ms (300 k) (emu/g, CoFe204)	He (300 k) (Oe)
CoFe$_2$O$_4$	16	7	11	–
CoFe$_2$O$_4$@Ag	4.8	11	3.3	72
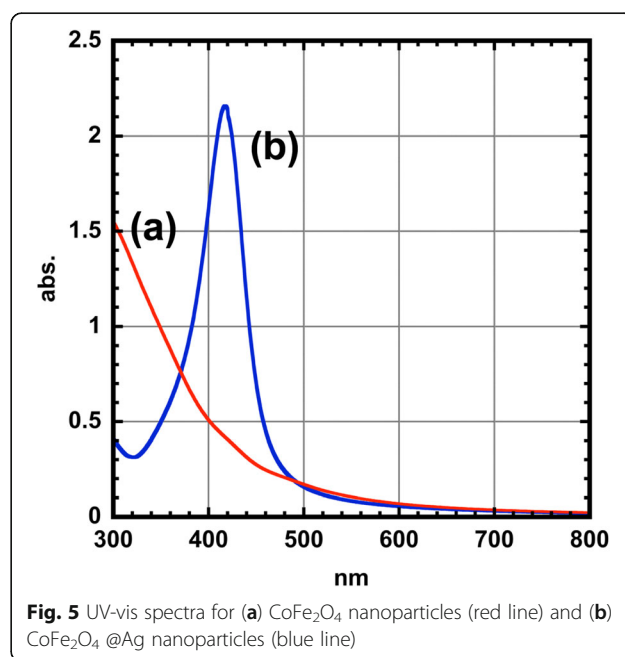
Fig. 5 UV-vis spectra for (**a**) CoFe$_2$O$_4$ nanoparticles (red line) and (**b**) CoFe$_2$O$_4$ @Ag nanoparticles (blue line)

Hara *et al. Nanoscale Research Letters* (2018) 13:176

Page 6 of 7

Fig. 6 Size distribution (**a**) of the $CoFe_2O_4$ (red line) and (**b**) the $CoFe_2O_4$@Ag nanoparticles (blue line) measured by DLS
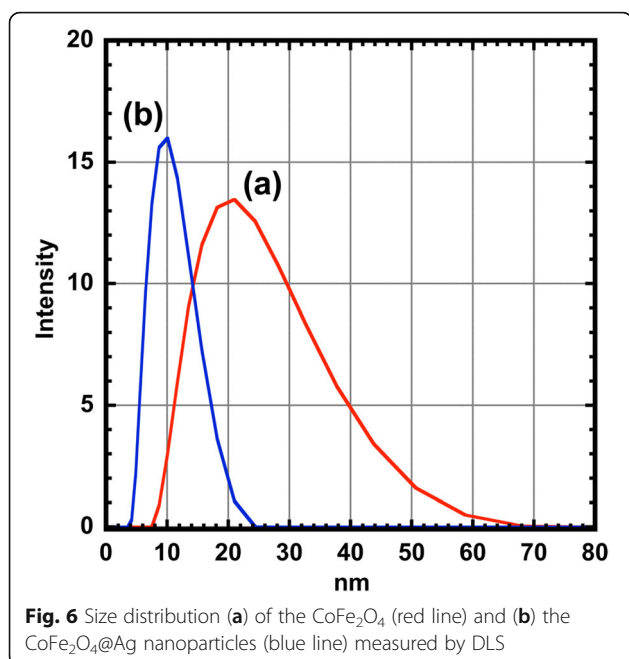
nanoparticles obtained from TEM, XRD, and DLS measurements are summarized in Table 2. The main difference in sizes measured by these two techniques is due to the presence of an adsorption layer consisting of the OA and OAm on the surface of the particles [35]. Organic compounds such as OA and OAm did not appear in TEM images due to the electron permeability (Fig. 1). Given that the chain lengths of the OA and the OAm are roughly 2 nm [36, 37], the size of $CoFe_2O_4$@Ag estimated by the TEM is slightly (ca. 4 nm) larger than that by the DLS. On the other hand, it is reasonable that the size of $CoFe_2O_4$ by the DLS is far larger than that estimated from this assumption. These results suggest that CoFe2O4 nanoparticles are agglomerated in hexane. This factor includes not only the size effect of the particles described above but also the low affinity between the $CoFe_2O_4$ surfaces and the protective agents. The tendency of agglomeration of the $CoFe_2O_4$ may not only due to the size effect of the particles described above but also due to the low affinity between the $CoFe_2O_4$ surfaces and the protective agents. Precipitation of $CoFe_2O_4$ nanoparticles was observed much more frequently than

Table 2 Summary of the sizes of NPs obtained from TEM, XRD, and DLS analysis

Nanoparticle	Size from TEM (nm)	Size from XRD (nm)	Size from DLS (nm) in hexane (PDI)
$CoFe_2O_4$	3.2 ± 0.76	7.1	19.67 (0.153)
$CoFe_2O_4$@Ag	5.3 ± 0.76	3.5	9.27 (0.083)

$CoFe_2O_4$@Ag nanoparticles in the process of redispersion by increasing the number of methanol washing. The high monodispersity of $CoFe_2O_4$@Ag is strongly supported by the low polydispersity index (PDI) obtained by the DLS measurements [38]. These results indicate that the coating with Ag adds not only an optical function but also the stability in solution to the $CoFe_2O_4$ nanoparticles.

Conclusions

The $CoFe_2O_4$@Ag nanoparticles synthesized by a simple and rapid one-pot process were found to be formed on having a uniform core-shell structure with a narrow size distribution from TEM images (Fig. 6). Also, these nanoparticles showed a multifunctionality consisting of the plasmonic light extinction property and a superparamagnetic behavior at room temperature. Furthermore, the core-shell nanoparticles showed higher H_c than $CoFe_2O_4$ nanoparticles at 5 K and 300 k. In addition, these nanoparticles maintained high monodispersity in an organic solvent. The uniform nanoparticles synthesized by the simple process have a great potential in various fields owing to the multifunctionality as well as the stability.

Additional File

Additional file1: Figure S1. (A) Model of core-shell nanoparticle. Calculated extinction spectra of the core-shell nanoparticle consisting of only the multipolar: (B) and dipolar plasmon modes: (C) surrounded by hexane ($n = 1.3740$). The dielectric value of core is varied: (a) 1, (b) 3, (c) 6, (d) 9, (e) 12, and (f) 15. (DOCX 110 kb)

Author details
[1]Department of Materials and Applied Chemistry, College of Science and Technology, Nihon University, 1-8-14 Kandasurugadai, Chiyoda-ku, Tokyo

Hara *et al. Nanoscale Research Letters* (2018) 13:176

Page 7 of 7

101-8308, Japan. [2]Department of Physics, College of Science and Technology, Nihon University, 1-8-14 Kandasurugadai, Chiyoda-ku, Tokyo 101-8308, Japan.

References

1. Park HY, Schadt MJ, Wang L, Lim IIS, Njoki PN, Kim SH, Jang MY, Luo J, Zhong CJ (2007) Fabrication of magnetic core @Shell Fe Oxide@ Au nanoparticles for interfacial bioactivity and bio-separation. Langmuir. 23(17): 9050–9056. https://doi.org/10.1021/la701305f

2. Wu W, He Q, Jiang C (2008) Magnetic iron oxide nanoparticles: Synthesis and surface functionalization strategies. Nanoscale Res Lett 3(11):397-415. https://doi.org/10.1007/s11671-008-9174-9

3. Kharisov BI, Dias HVR, Kharissova OV, Vázquez A, Peña Y, Gómez I (2014) Solubilization, dispersion and stabilization of magnetic nanoparticles in water and non-aqueous solvents: recent trends. RSC Adv 4(85):45354-45381. https://doi.org/10.1039/C4RA06902A

4. Du M, Liu Q, Huang C, Qiu X (2017) One-step synthesis of magnetically recyclable Co@BN core–shell nanocatalysts for catalytic reduction of nitroarenes. RSC Adv 7(56):35451–35459. https://doi.org/10.1039/C7RA04907B

5. Wang L, Luo J, Fan Q, Suzuki M, Suzuki IS, Engelhard MH, Lin Y, Kim N, Wang JQ, Zhong C-J (2005) Monodispersed core-shell Fe3O4@Au nanoparticles. J Phys Chem B 109(46):21593–21601. https://doi.org/10.1021/jp0543429

6. Kelly AT, Filgueira CS, Schipper DE, Halas NJ, Whitmire KH (2017) Gold coated iron phosphide core–shell structures. RSC Adv. 7(42):25848–25854. https://doi.org/10.1039/C7RA01195D

7. Garcia-Torres J, Vallés E, Gómez EJ (2010) Synthesis and characterization of Co@Ag core-shell nanoparticles. J Nanoparticle Res 12(6):2189–2199. https://doi.org/10.1007/s11051-009-9784-x

8. Xu Z, Hou Y, Sun SJ (2007) Magnetic core/shell Fe3O4/Au and Fe3O 4/Au/ Ag nanoparticles with tunable plasmonic properties. J Am Chem Soc 129(28):8698–8699. https://doi.org/10.1021/ja073057v

9. Mandal M, Kundu S, Ghosh SK, Panigrahi S, Sau TK, Yusuf SM, Pal TJ (2005) Magnetite nanoparticles with tunable gold or silver shell. J Colloid Interface Sci. 286(1):187–194. https://doi.org/10.1016/j.jcis.2005.01.013

10. Lu L, Zhang W, Wang D, Xu X, Miao J, Jiang Y (2010) Fe@Ag core-shell nanoparticles with both sensitive plasmonic properties and tunable magnetism. Mater Lett 64(15):1732–1734. https://doi.org/10.1016/j.matlet.2010.04.025

11. Ferjaoui Z, Schneider R, Meftah A, Gaffet E, Alem H (2017) Functional responsive superparamagnetic core/shell nanoparticles and their drug release properties. RSC Adv 7(42):26243–26249. https://doi.org/10.1039/c7ra02437a

12. Nairan A, Khan U, Iqbal M, Khan M, Javed K, Riaz S, Naseem S, Han X (2016) Structural and Magnetic Response in Bimetallic Core/Shell Magnetic Nanoparticles. Nanomaterials. 6(4):72. https://doi.org/10.3390/nano6040072

13. Song Q, Zhang ZJJ (2004) Shape Control and Associated Magnetic Properties of Spinel Cobalt Ferrite Nanocrystals. J Am Chem Soc 126(19): 6164–6168. https://doi.org/10.1021/ja049931r

14. Tsai C-F, Chen L, Chen A, Khatkhatay F, Zhang W, Wang H (2013) Enhanced Flux Pinning Properties in Self-Assembled Mangetic CoFe2O4 Nanoparticles Doped YBa2Cu3O7–δ Thin Films. IEEE Trans Appl Supercond 23(3):8001204.

15. Chen D, Yi X, Chen Z, Zhang Y, Chen B, Kang Z (2014) Synthesis of CoFe2O4 nanoparticles by a low temperature microwave-assisted ball-milling technique. Int J Appl Ceram Technol 11(5):954–959. https://doi.org/10.1111/ijac.12110

16. Chinnasamy CN, Jeyadevan B, Shinoda K, Tohji K, Djayaprawira DJ, Takahashi M, Justin Joseyphus R, Narayanasamy A (2003) Unusually high coercivity and critical single-domain size of nearly monodispersed CoFe2O4 nanoparticles. Appl Phys Lett 83(14):2862–2864. https://doi.org/10.1063/1.1616655

17. López-Ortega A, Lottini E, Fernández CDJ, Sangregorio C (2015) Exploring the Magnetic Properties of Cobalt-Ferrite Nanoparticles for the Development of a Rare-Earth-Free Permanent Magnet. Chem Mater 27(11): 4048–4056. https://doi.org/10.1021/acs.chemmater.5b01034

18. Sun S, Zeng H, Robinson DB, Raoux S, Rice PM, Wang SX, Li GJ (2004) Monodisperse MFe 2 O 4 (M = Fe, Co, Mn) Nanoparticles. J Am Chem Soc 126(1):273–279. https://doi.org/10.1021/ja0380852

19. Song Y, Ding J, Wang Y (2012) Shell-dependent evolution of optical and magnetic properties of Co@Au core-shell nanoparticles. J Phys Chem C 116(20):11343–11350. https://doi.org/10.1021/jp300118z

20. Wang L, Park H-Y, Lim SI-I, Schadt MJ, Mott D, Luo J, Wang X, Zhong C-JJ (2008) Core@shell nanomaterials: gold-coated magnetic oxide nanoparticles. J Mater Chem 18(23):2629. https://doi.org/10.1039/b719096d

21. Sharma SK, Vargas JM, Vargas NM, Castillo-Sepúlveda S, Altbir D, Pirota KR, Zboril R, Zoppellaro G, Knobel MR (2015) Unusual magnetic damping effect in a silver–cobalt ferrite hetero nano-system. R Soc Chem Adv 5:17117–17122. https://doi.org/10.1039/C4RA14960B

22. Kooti M, Saiahi S, Motamedi HJ (2013) Fabrication of silver-coated cobalt ferrite nanocomposite and the study of its antibacterial activity. J Magn Magn Mater 333:138–143. https://doi.org/10.1016/j.jmmm.2012.12.038

23. Zhang K, Xiang Y, Wu X, Feng L, He W, Liu J, Zhou W, Xie S. (2009) Enhanced Optical Responses of Au @ Pd Core / Shell Nanobars 8:1162–1168

24. Mätzler, C (2002) MATLAB Functions for Mie Scattering and Absorption. IAP Res Rep 2002-08(July 2002):1139–1151. https://doi.org/10.1039/b811392k

25. Ordal MA, Bell, R. J, Alexander RW, Long LL, Querry MR (1985) Optical properties of fourteen metals in the infrared and far infrared: Al, Co, Cu, Au, Fe, Pb, Mo, Ni, Pd, Pt, Ag, Ti, V, and W. 24(24):4493–4499

26. Wu W, Wu Z, Yu T, Jiang C, Kim WS (2015) Recent progress on magnetic iron oxide nanoparticles: Synthesis, surface functional strategies and biomedical applications. Sci Technol Adv Mater. 16(2). https://doi.org/10.1088/1468-6996/16/2/023501

27. Stefan M, Leostean C, Pana O, Soran ML, Suciu RC, Gautron E, Chauvet O (2014) Synthesis and characterization of Fe3O4@ZnS and Fe3O4@Au@ZnS core-shell nanoparticles. Appl Surf Sci 288:180–192. https://doi.org/10.1016/j.apsusc.2013.10.005

28. Tang R, Jiang C, Qian W, Jian J, Zhang X, Wang H, Yang H (2015) Dielectric relaxation, resonance and scaling behaviors in Sr3Co2Fe24O41 hexaferrite. Sci Rep 5:1–11. https://doi.org/10.1038/srep13645

29. Sun Y, Ji G, Zheng M, Chang X, Li S, Zhang YJ (2010) Synthesis and magnetic properties of crystalline mesoporous CoFe 2 O 4 with large specific surface area. J Mater Chem 20(5):945–952. https://doi.org/10.1039/B919090B

30. Bohara RA, Thorat ND, Yadav HM, Pawar SH (2014) One-step synthesis of uniform and biocompatible amine functionalized cobalt ferrite nanoparticles: a potential carrier for biomedical applications. New J Chem 38(7):2979. https://doi.org/10.1039/c4nj00344f

31. Pervaiz E, Humaira IHG (2015) Hydrothermal Synthesis and Characterization of CoFe 2 O 4 Nanoparticles and Nanorods. J Appl Phys 117. https://doi.org/10.1007/s10948-012-1749-0

32. Park J, Lee E, Hwang N-M, Kang M, Kim SC, Hwang Y, Park J-G, Noh H-J, Kim J-Y, Park J-H, Hyeon T (2005) One-Nanometer-Scale Size-Controlled Synthesis of Monodisperse Magnetic Iron Oxide Nanoparticles. Angew Chemie Int Ed 44(19):2872–2877. https://doi.org/10.1002/anie.200461665

33. Wang C, Xu J, Wang J, Rong Z, Li P, Xiao R, Wang S (2015) Polyethylenimine-interlayered silver-shell magnetic-core microspheres as multifunctional SERS substrates. J Mater Chem C 3(33):8684–8693. https://doi.org/10.1039/C5TC01839K

34. Walker JM, Zaleski JM (2016) A simple route to diverse noble metal-decorated iron oxide nanoparticles for catalysis. Nanoscale 8(3):1535–1544. https://doi.org/10.1039/C5NR06700F

35. Lim J, Yeap S, Che H, Low S (2013) Characterization of magnetic nanoparticle by dynamic light scattering. Nanoscale Res Lett 8(1):381. https://doi.org/10.1186/1556-276X-8-381

36. Wang Z, Wen X-D, Hoffmann R, Son JS, Li R, Fang C-C, Smilgies D-M, Hyeon T (2010) Reconstructing a solid-solid phase transformation pathway in CdSe nanosheets with associated soft ligands. Proc Natl Acad Sci 107(40):17119–17124. https://doi.org/10.1073/pnas.1011224107

37. Zhang L, He R, Gu HC (2006) Oleic acid coating on the monodisperse magnetite nanoparticles. Appl Surf Sci 253(5):2611–2617. https://doi.org/10.1016/j.apsusc.2006.05.023

38. Araújo-Neto RP, Silva-Freitas EL, Carvalho JF, Pontes TRF, Silva KL, Damasceno IHM, Egito EST, Dantas AL, Morales MA, Carriço ASJ (2014) Monodisperse sodium oleate coated magnetite high susceptibility nanoparticles for hyperthermia applications. J Magn Magn Mater 364:72–79. https://doi.org/10.1016/j.jmmm.2014.04.001